Solidification Processes and Microstructures: A symposium in honor of Wilfried Kurz *Edited by M. Rappaz*
TMS (The Minerals, Metals & Materials Society), Charlotte, NC, March 15-18, 2004, pp. 33-39

SIMULATION OF SHRINKAGE AND STRESS IN SOLIDIFYING STEEL SHELLS OF DIFFERENT GRADES

Ya Meng, Chunsheng Li, Jon Parkman, and Brian G. Thomas

University of Illinois at Urbana-Champaign
Department of Mechanical & Industrial Engineering,
1206 West Green St., Urbana, IL 61801

Keywords: Computation, thermo-mechanical models, continuous casting, steel, heat flux, solidification, shrinkage, carbon content, SSCT test, taper, steel grade

Abstract

Thermal–mechanical behavior of the solidifying shell is important for design of taper and understanding crack formation and other defects during continuous casting of steel. A transient finite-element model, CON2D, has been developed to simulate the evolution of temperature, stress and strain in the solidifying shell during this process. The model features unified elastic-viscoplastic constitutive models for austenite, ferrite, mushy, and liquid steel. The model was validated by simulating an SSCT experiment similar to that of Kurz. CON2D was then applied to investigate the effect of steel grade on thermo-mechanical behavior of a slice domain under realistic heat flux conditions. The shrinkage predicted by CON2D was compared with simpler methods, such as that of Dippenaar. This simple method is found to over-estimate the shrinkage of low carbon steels, where a substantial fraction of soft delta-ferrite exists, but matches reasonably for high carbon steel, containing strong austenite. Implications of the stress and strain profiles in the solidifying steel and practical applications are also discussed.

Introduction

The shrinkage associated with solidification and cooling is of practical importance for many casting processes, as it affects both the casting dimensions and the formation of hot tear cracks, and other defects in the product. In continuous casting processes, molds are often tapered to match the shrinkage, in order to continuously support the weak shell and avoid defects. Taper design depends on accurately quantifying the fundamental phenomena that govern shrinkage during the formation and cooling of a solidifying shell.

This paper summarizes recent work with computational models to predict these phenomena for steel, during the continuous casting process. The model is first validated by comparison with measurements of a "Submerged Split Chill Tensile" (SSCT) test. This important measurement tool was pioneered by Kurz[1] to study mechanical behavior and failure phenomena during solidification. The model is then applied to predict shrinkage during continuous casting of steel, investigating the effect of grade. Finally, simplified models to predict shrinkage are evaluated.

Shrinkage Models

A finite-element elastic-viscoplastic thermal-stress model, CON2D[2-4] has been developed to predict thermal-mechanical behavior of steel during continuous casting, including shrinkage of the solidifying steel shell. The model results have many applications, such as for designing the taper of the narrow faces of a continuous casting mold for steel slabs, in order to accommodate shrinkage of the wide faces, as shown in Fig. 1.[5] The model solves a 2D finite-element discretization of the transient heat conduction equation in a Lagrangian reference frame that moves down through the caster with the solidifying steel shell. Next, the force equilibrium, constitutive, and strain displacement equations are solved under a condition of generalized plane strain in both the width and casting directions[2]. Thermal and mechanical behavior are studied here in a longitudinal slice through the centerline of the shell (Fig. 2). This slice domain has been shown to be an accurate and economical method to approximate shrinkage of the thin solidifying shell in the mold, despite the corner effects[6].

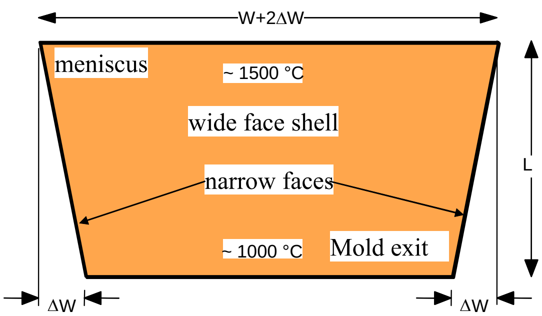

Fig. 1: Wide face shrinkage and narrow face taper

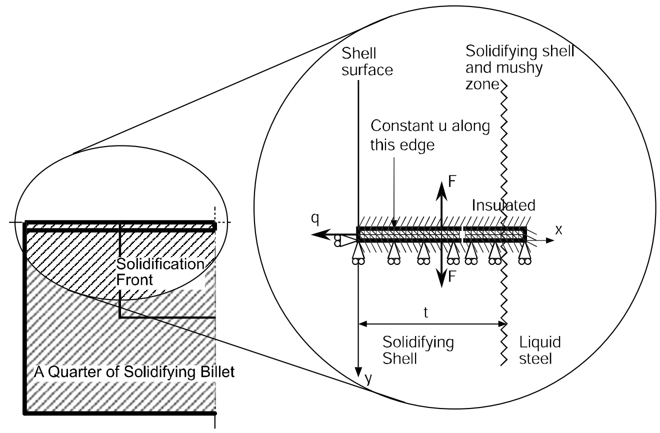

Fig. 2: 1-D Slice Simulation Domain for CON2D

Simple Shrinkage Predictions

Owing to the great computational effort required for a complete finite-element stress simulation, and the dominance of thermal strain in the shrinkage, simpler ways are sought to estimate shrinkage from the computed temperature histories of points in the shell. Recent work with CON1D[7] compares two simple methods. First, thermal strain ε_{th1} can be estimated simply from the shell surface temperature, T_s:

$$\varepsilon_{th1} = TLE(T_{sol}) - TLE(T_s) \qquad [1]$$

where *TLE* is the thermal linear expansion function for a given steel, Fig. 3, calculated from weighted averages of the phases present.

Another method, developed by Dippenaar[8] computes the strain ε_{th2}, by summing the average *TLE* of the solid portion of the shell between each pair of consecutive time steps:

$$\varepsilon_{th2} = \sum_{t=0}^{t}\left(\left(\frac{1}{i}\right)\sum_{i=1}^{solid\ nodes}\left(TLE\left(T_i^t\right) - TLE\left(T_i^{t+\Delta t}\right)\right)\right) \qquad [2]$$

where the shell thickness is divided into i sections.

CON2D Stress Model

In the elastic-viscoplastic finite-element model, the total strain is decomposed into elastic, thermal, inelastic and flow-strain components. Thermal strain dominates the total, and depends on temperature and steel grade, as shown in Fig. 3. A simple micro-segregation model is adopted to track the weight fractions of each phase[7]. Unified plastic-creep constitutive models are used to capture the temperature, strain-rate, phase fraction, and grade sensitivity of steel strength at high temperature. The instantaneous equivalent inelastic strain rate depends on the current equivalent stress, temperature, the carbon content, and the current equivalent inelastic strain, which accumulates below the solidus temperature. When the steel is mainly austenite phase, (%γ >90%), Model III by Kozlowski[9] was applied. This function matches tensile test measurements of Wray[10] and creep test data of Suzuki[11]. When the steel contains significant amounts of soft delta-ferrite phase (%δ >10%), a power-law model is used[4], which matches measurements of Wray above 1400 ^{o}C[12]. Fig. 4 shows the accuracy of the constitutive model predictions compared with stresses measured by Wray[10] at 5% strain at different strain rates and temperatures. This figure also shows the higher relative strength of austenite, which is important for shrinkage of the solidifying shell, and greatly affects the grade dependence of

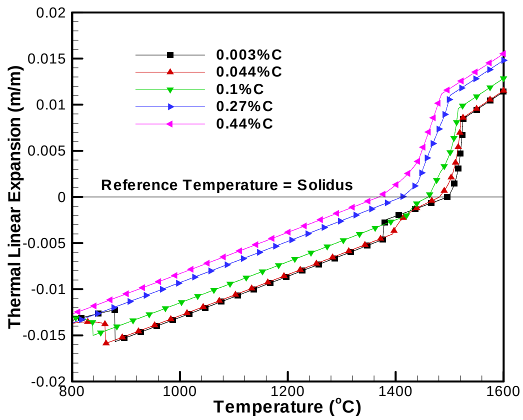

Fig. 3: Thermal expansion of steel, *TLE(T)*

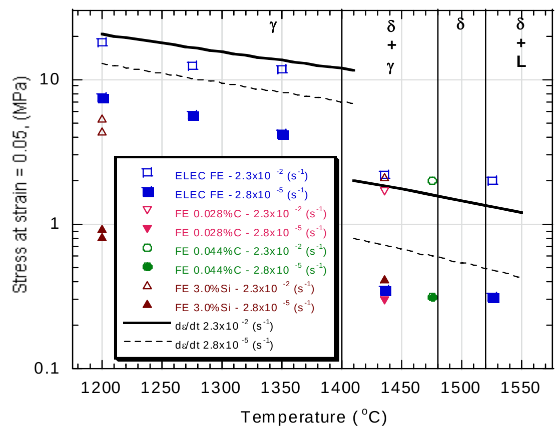

Fig. 4: Steel strength at high temperature (comparing predicted and measured values for α and γ)

ideal taper. Further details regarding the model formulation are presented elsewhere, including its extensive validation with both analytical solutions and plant measurements[4, 6].

<u>Model Validation: Submerged Split Chill Tensile (SSCT) Test</u>

To further validate the model, it was applied to simulate an SSCT test (Fig.5). The SSCT test was pioneered by Kurz and coworkers[1, 13] to measure metal strength during solidification by applying a tensile force perpendicular to the columnar dendrite growth direction. The measured change in position of the lower half of the copper chill is shown in Fig. 6, as it is lowered into a bath of 0.25%C steel, held for 12s, and then pulled away from the upper half[13]. During the submergence and holding time, thermal expansion of the upper half of the chill exerts a tensile force on the solidifying shell. Shrinkage of the solidifying steel shell adds to this force. This pushes the lower half downward, while the applied force measured at the load cell remains at zero, owing to force control. At the end of the 12s holding time, the test switches from force control to position control. At the beginning of the tensile test (after the hold) the lower half moves downward at a controlled velocity. When movement starts, the force is redefined to zero.

The SSCT test was simulated with a 0.5 x 25mm slice through the solidifying shell. Heat flux at the chill / steel interface is taken from thermocouple measurements and was adjusted so that predicted shell growth roughly matched the measurement. The domain was kept flat by constraining the vertical displacements along the upper side of the mesh to the same position-time profile, chosen to mimic the position – time results in Fig. 6. Specifically, during the first 2.7s after submergence, the position moves 0.23 mm (0.0023 s^{-1} strain rate, based on the chill height of 37mm). The strain rate dropped to 0.0004 s^{-1} for the remaining 9.3s of the hold. Finally, a strain rate of 0.046 s^{-1} was applied during the tensile test time.

If there was no axial force exerted on the shell, then the stress profile of Fig. 7 would be produced. Note the surface would be in compression with the interior in tension, where hot tears could form. Stress would drop to the ferrostatic pressure (near zero) in the liquid. However, the expansion forces the entire shell into tension. The simulated and measured force versus time curves are compared in Fig. 8. True force on the shell was not measured prior to the hold time so the simulation starts at 12s. Similarly, the time of applied load is offset to measure from the time of initial submergence in both cases. Before the test officially starts, the model predicts force to grow during the hold time. After the tensile test begins, both model and measurement show a steep force increase. The measurement later relaxes to a constant before declining just before the test ends. This is likely due to gradual failure of the shell due to hot tearing and strain localization. This is not simulated, so the model overpredicts subsequent force in the shell. Solidification during the test allows the shell to maintain a load even after it starts to fail. The strain to failure is difficult to determine, as it includes strain both before and after the test starts. Thus, the combination of sophisticated experimental measurements and advanced modeling of the experiments is the best way to understand the fundamentals of mechanical behavior during solidification. Considering the simplifications and uncertainties, the model is reasonably able to predict mechanical behavior during solidification, prior to crack formation.

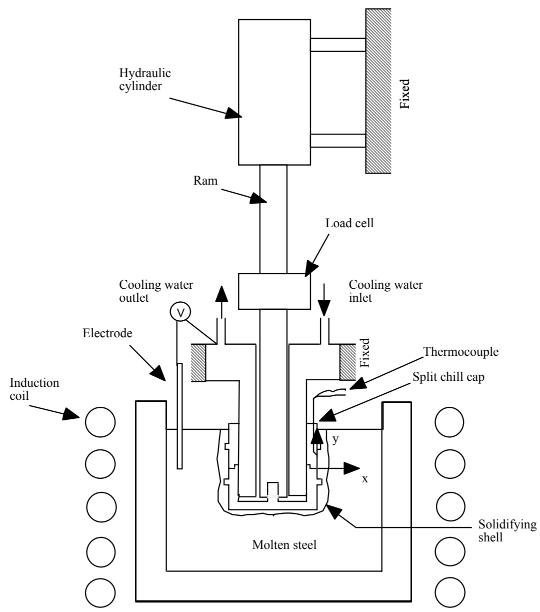

Fig. 5: Submerged Split Chill Tensile (SSCT) apparatus[1, 13]

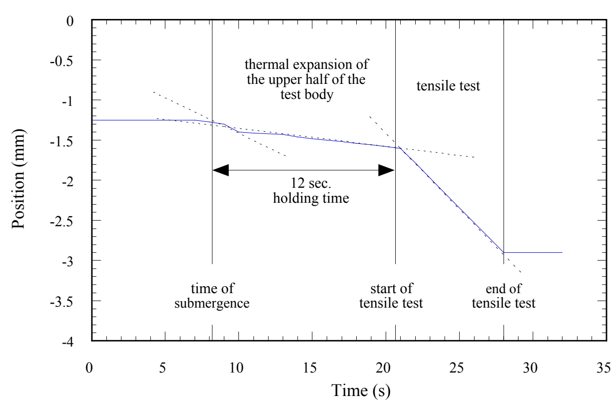

Fig. 6: Typical SSCT test data

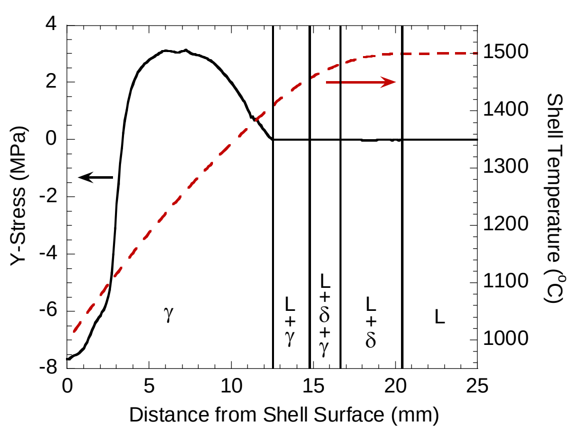

Fig. 7: Typical temperature and stress profiles predicted through shell thickness.

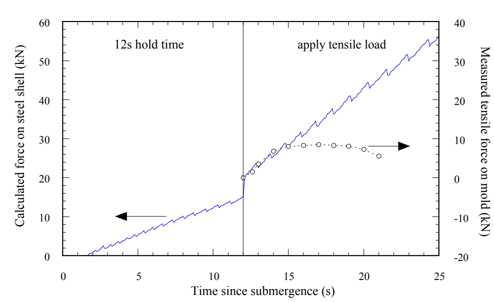

Fig. 8: Comparison of measured and simulated force during SSCT test

Results

The shrinkage models are applied to simulate the solidifying shell during continuous casting of steel slabs. In particular, the effect of steel grade is investigated.

Heat Flow Model

Heat flux leaving the surface of the solidifying shell is calculated using a finite-difference model of shell solidification, CON1D, that features detailed treatment of the slag layers in the interfacial gap, coupled to a 2-D computation of mold heat conduction[7]. Constants in the model, such as contact resistances, powder consumption rate, flux properties, and solid flux velocity, dictate the heat flux profile down the mold. Through calibration, the total heat flux (integrated from the heat flux profile) was forced to match Eq. 3[14], which was obtained from a curve fit of many measurements under different conditions at a typical slab caster.

$$Q_G = 4.63 \cdot 10^6 \mu^{-0.09} T_{flow}^{-1.19} V_C^{0.47} \left\{ 1 - 0.152 \exp\left[-\left(\frac{0.107 - \%C}{0.027} \right)^2 \right] \right\} \qquad [3]$$

where Q_G is the mean heat flux (MW/m^2), μ is the powder viscosity at 1300 °C, (0.083 Pa-s for flux E and 0.192 Pa-s for flux C), T_{flow} is the melting temperature of the mold flux (1120 °C for flux E and 1215 °C for flux C), V_c is the casting speed (1.5 m/min), and %C is carbon content.

Heat flux and surface temperature predictions are presented in Figs. 9 and 10 for steel grades with a range of carbon contents. These results quantify the well-known fact that heat flux drops for peritectic steels (near .107%C). Heat flux drops even further for peritectic steels because they generally use mold powders like C with high solidification temperatures, (which hence form a thicker insulating flux layer against the mold wall)[5, 7]. Surface temperature is naturally lower for the higher heat flux.

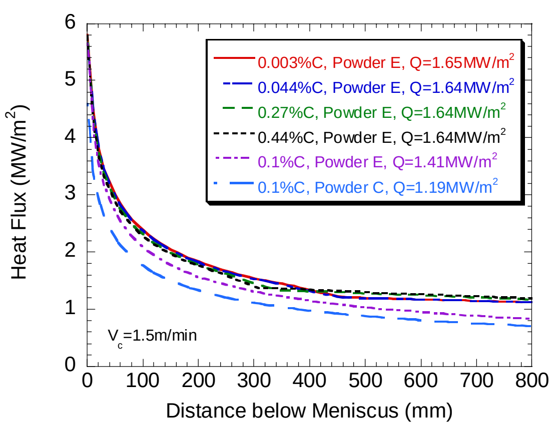

Fig. 9: Heat flux predicted down mold

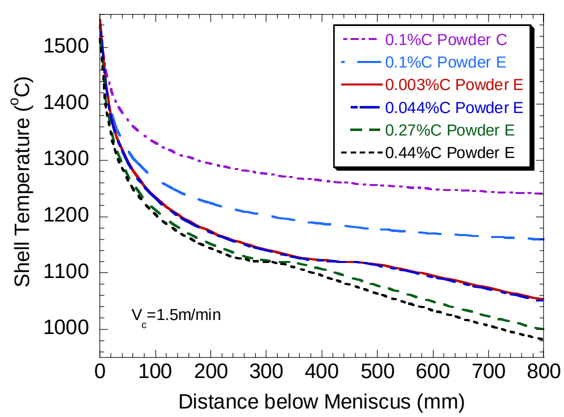

Fig. 10: Predicted surface temperature profiles

Shrinkage Predictions

Shrinkage and stress predictions were made using the CON2D model, assuming ideal taper conditions (implying free shrinkage of the shell in the mold). The temperature and stress profiles through the shell are shown in Fig. 11 for a peritectic steel (0.1%C). Compared with the higher carbon steel in Fig. 7, the stresses near the solidification front are lower, owing to the extra creep of the weak delta-ferrite phase. The effect of steel grade on shrinkage is shown in Fig. 12. Lower surface temperature increases the amount of shrinkage. This effect appears to outweigh the importance of the extra shrinkage (higher *TLE*) experienced by peritectic steels. Thus, peritectic steels experience less shrinkage and require less taper than either low or high carbon steels. The low carbon steels experience both heat flux and shell shrinkage that is greater than for the other grades.

The simple Dippanaar method 2 for predicting shrinkage performs well for higher carbon steel, as it matches the advanced CON2D model predictions in Fig.14. However, the low carbon steels (<.16 %C) have extra inelastic strain, owing to their microstructure being in the soft, rapidly creeping delta phase. This extra creep generated in the solid tends to lower the amount of shrinkage experienced by these grades. This explains the big overprediction of method 2 for these grades, observed in Fig. 13. The simple shrinkage prediction method 1 (based on surface-temperature) consistently underpredicts the shrinkage, because it neglects the compression generated in the surface.

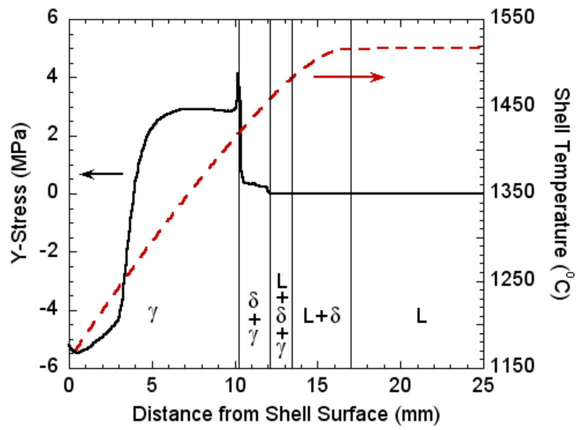

Fig. 11: Stress Profile through shell

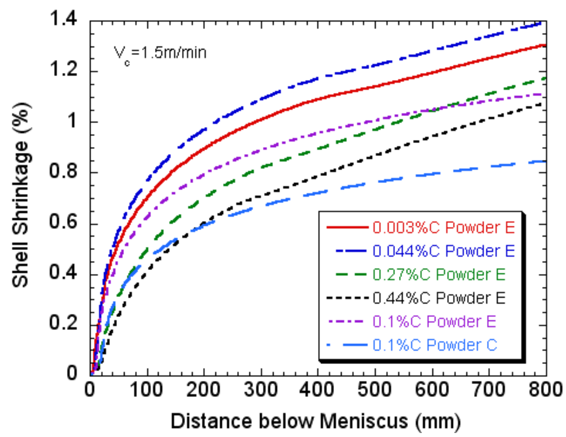

Fig. 12: CON2D Shrinkage predictions

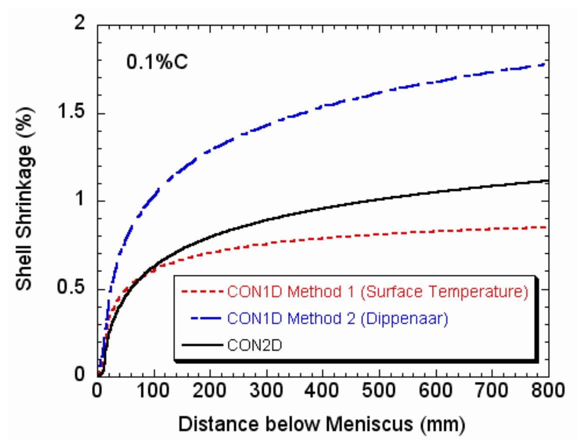

Fig. 13: Typical shrinkage profile comparison for low and medium-carbon steels (Powder E)

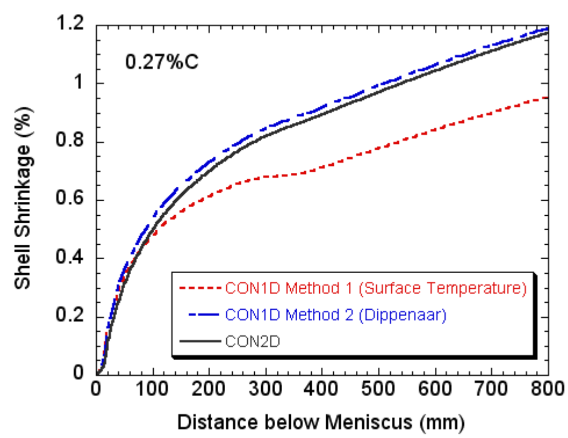

Fig. 14: Typical shrinkage profile comparison predicted for high-carbon steel

Applications

A finite-element model CON2D to predict thermo-mechanical behavior of the shell during solidification has been developed and validated. This model has recently been applied to a variety of practical problems:

1) predicting ideal taper during slab[5] and billet casting,[6]
2) understanding the effect of corner radius on longitudinal cracks in the mold,
3) finding the minimum shell thickness at mold exit to avoid breakout,[15] and
4) finding the maximum casting speed to still avoid bulging and off-corner longitudinal cracks below the mold.[4]

Acknowledgements

The authors wish to thank the Continuous Casting Consortium, and the National Center for Supercomputing Applications.

References

1. P. Ackermann, W. Kurz and W. Heinemann: "In Situ Tensile Testing of Solidifying Aluminum and Al-Mg Shells", *Materials Science and Engineering,* 1985, (75), pp. 79-86.
2. A. Moitra and B.G. Thomas: "Application of a Thermo-Mechanical Finite Element Model of Steel Shell Behavior in the Continuous Slab Casting Mold", *76th Steelmaking Conference*, (Dallas, TX, 28-31 Mar. 1993), 1993, vol. 76, pp. 657-67.
3. B.G. Thomas and H. Zhu: "Thermal Distortion of Solidifying Shell Near Meniscus in Continuous Casting of Steel", *JIM/TMS Solidfication Science and Processing Conference*, (Honolulu, HI, Dec. 13-15, 1995), 1995, pp. 197-208.
4. C. Li and B.G. Thomas: "Maximum casting speed for continuous cast steel billets based on sub-mold bulging computation", *85th Steelmaking Conference*, (Nashville, TN, USA, 10-13 Mar. 2002), vol. 85, pp. 109-30.
5. B.G. Thomas and C. Ojeda: "Ideal Taper Prediction for Slab Casting", *ISSTech Steelmaking Conference*, (Indianapolis, IN, USA, April 27-30, 2003), 2003, vol. 86, pp. 396-08.
6. C. Li and B.G. Thomas: "Ideal Taper Prediction for Billet Casting", *ISSTech Steelmaking Conference*, (Indianapolis, IN, USA, April 27-30, 2003), 2003, vol. 86, pp. 685-700.
7. Y. Meng and B.G. Thomas: "Heat Transfer and Solidification Model of Continuous Slab Casting: CON1D", *Metall. Mater. Trans. B (USA),* 2003, vol. 34B (5), pp. 685-705.
8. R.J. Dippenaar, I.V. Samarasekera and J.K. Brimacombe: "Mold Taper in Continuous Casting Billet Machines", *ISS Transactions,* 1986, (7), pp. 31-43.
9. P. Kozlowski, B.G. Thomas, J. Azzi and H. Wang: "Simple Constitutive Equations for Steel at High Temperature", *Metall. Trans. A,* 1992, vol. 23A (3), pp. 903-18.
10. P.J. Wray: "Plastic Deformation of Delta-Ferritic Iron at Intermediate Strain Rates", *Metall. Trans. A,* 1976, vol. 7A (Nov.), pp. 1621-27.
11. T. Suzuki, K.H. Tacke, K. Wunnenberg and K. Schwerdtfeger: "Creep Properties of Steel at Continuous Casting Temperatures", *Ironmaking and Steelmaking,* 1988, vol. 15 (2), pp. 90-100.
12. B.G. Thomas, A. Moitra and R. McDavid: "Simulation of longitudinal off-corner depressions in continuously cast steel slabs", *Iron and Steelmaker (USA),* 1996, vol. 23 (4), pp. 57-70.
13. C. Bernhard, H. Hiebert and M.M. Wolf: "Simulation of shell strength properties by the SSCT test", *ISIJ International (Japan),* 1996, vol. 36 (Suppl. Science and Technology of Steelmaking), pp. 163-66.
14. C. Cicutti, M. Valdez, T. Perez, G.D. Gresia, W. Balante and J. Petroni: "Mould thermal evaluation in a slab continuous casting machine", *85th Steelmaking Conference*, (Nashville, TN, USA, 10-13 Mar. 2002), vol. 85, pp. 97-107.
15. C. Li and B.G. Thomas: "Analysis of the potential productivity of continuous cast molds", *The Brimacombe Memorial Symposium*, (Vancouver, British Columbia, Canada, 1-4 Oct. 2000), Canadian Institute of Mining, Metallurgy and Petroleum, Montreal PQ, Canada, 2000, pp. 595-611.